



Modelling of high impedance faults in distribution systems and validation based on multiresolution techniques[☆]

Vicente Torres-García^a, Daniel Guillen^{b,*}, Jimena Olveres^c,
Boris Escalante-Ramírez^c, Juan R. Rodríguez-Rodríguez^a

^a Departamento de Energía Eléctrica, Universidad Nacional Autónoma de México, Ciudad de México, México

^b Escuela de Ingeniería y Ciencias, Tecnológico de Monterrey, Nuevo León, México

^c Departamento de Procesamiento de Señales, Universidad Nacional Autónoma de México, Ciudad de México, México

ARTICLE INFO

Article history:

Received 6 September 2019

Revised 4 February 2020

Accepted 6 February 2020

Available online 19 February 2020

Keywords:

Detection

Fault current

Feature selection

High impedance fault

Hermite transform

Multiresolution

Wavelet transform

ABSTRACT

The electric arc phenomenon associated with high impedance faults (HIFs) in distribution systems is an exciting subject that directly impacts over the reliability of electrical utilities, because fault currents are very small and present non-linearity and asymmetrical waveforms. Therefore, HIFs may be an undetectable phenomenon by overcurrent protections like fuses, re-closers, and relays. A HIF entails a challenge for its detection and location. In this sense, more realistic high impedance models, as well as reliable signal processing techniques, are needed to extract all transient characteristics aiming to detect HIFs in distribution networks. In this work, an efficient Resistive-HIF model is proposed and implemented into the Alternative Transients Program of the Electromagnetic Transients Program (ATP/EMTP) software to represent the main characteristics of HIFs. The model is compared against well-prove models by using two multiresolution approaches based on the Hermite transform and the Wavelet transform considering different frequency bands.

© 2020 Elsevier Ltd. All rights reserved.

1. Introduction

When an overhead power line physically breaks out and falls to the ground, or makes contact with the ground through any object, it leads to a well-known concept called high impedance faults. A HIF is frequently accompanied by an electric arc, which can result in fire hazards, damage to the electrical equipment or risk to human life. According to the Power System Relaying and Control Committee of the Institute of Electrical and Electronics Engineers (IEEE PSRC), a HIF is defined as an unwanted electrical contact of an energized conductor with a non-conductive surface (sod, grass, tree branches, asphalt or concrete), which limits the fault current to a lower level. Consequently, it is undetectable by the conventional overcurrent protection [1]. These are the reasons why HIF detection and its location have presented an important concern for the protection engineering, remaining as an unsolved problem yet.

[☆] This paper is for regular issues of CAEE. Reviews processed and recommended for publication to the Editor-in-Chief by Associate Editor Dr. F. Piccialli.

* Corresponding author.

E-mail addresses: v.torres.1982@fi-b.unam.mx (V. Torres-García), guillenad@tec.mx (D. Guillen), jolveres@cvicom.unam.mx (J. Olveres), boris@unam.mx (B. Escalante-Ramírez), jr_rodriguez@fi-b.unam.mx (J.R. Rodríguez-Rodríguez).

The purpose of studying the HIF phenomenon is to reduce the danger of placing people at risk due to the arc involved. In this sense, many HIF models have been proposed in the literature to understand this issue aiming to enhance its analysis, detection and location. For example, the first reported model was based on measurements considering a low-frequency spectrum [2]. This model takes into account two diodes and two direct current (d.c.) voltage sources to define the HIF characteristics. Harnessing the advantages of this model, other works have improved it by adding linear resistances and inductances [3]. On the other hand, more detailed models may generate a better representation of the physical conditions during HIFs, where non-linear resistances are included in the diodes-based model [4]. HIF models based on time-varying non-linear resistances were proposed to simulate the non-linearity and the asymmetry of the voltage-current characteristics. Those models consider one cycle of steady-state during the fault period, and also include the build-up and shoulder characteristics of the current waveform, which is obtained from the transient state (period of fault) [5]. There are also models defined by the thermal equations of the arc, supported by the Mayr and Cassie equations [6]; in this kind of model, the arc model parameters and high resistance values are determined by using experimental measurements.

A Kalman filter-based technique has been applied to detect variations in the fundamental frequency of the fault current and its harmonics produced [7], which may represent an indicative of HIFs. Moreover, time-frequency analysis based on the discrete wavelet transform (DWT) has been proposed, because this technique allows a qualitative and quantitative multiresolution analysis, facilitating the HIF detection [8,9]. Additionally, a method based on Gabor transform (GT) and Wigner distribution (WD) was introduced to detect HIFs [10]. Another contribution of a mathematical approach based on orthogonal component decomposition technique has been adopted for HIF detection in [11], also an evidential reasoning-based algorithm to detect and distinguish switching events from HIFs is reported in [12]. In [13], decision trees (DT) and extended Kalman filter (EKF) are used to estimate the harmonic content of the fault current aiming to detect HIFs.

Another issue of HIFs is their location where different techniques have been explored. For instance, in [3], a new analytic formulation of HIF location, by employing a least square-based estimator is proposed. In [14], power line communication (PLC) devices are used to locate HIFs; this method calculates the impedance at various frequencies to estimate the fault location. Another work addressed the subject of HIF location to identify the faulted section [15], where the faulted section is obtained using ranking analysis and DWT. Another approach based on DWT was proposed in [16] to find the faulted section, the average of the absolute difference between the extracted features was compared against the stored features, where the lowest differences are used to identify the faulted section. In [17], a new methodology for detection and area location of HIFs on unbalanced distribution systems is introduced. The method is called quasi-differential zero sequence protection (PQDSZ), and it can detect HIFs by analyzing the zero-sequence current. Recently, a technique based on time-domain analysis was proposed in [18], showing excellent performance during the fault location process of HIFs in distribution networks.

Therefore, to get a reliable detection and location of HIFs, more detailed models are essential to adequately represent the phenomenon of low current amplitude and electric arc, harmonic and non-harmonic components as well as avoiding erratic arc current waveforms. In this paper, a resistive-HIF model considering a non-linear resistance is proposed. Its performance is compared with the diodes-based model, and a multiresolution analysis is carried out using the Hermite transform (HT) and the wavelet transform (WT) to assess all transient information produced by both models. The multiresolution analysis will be done aiming to prove its effectiveness because all high-frequency components define the detection of HIFs in distribution networks, being this the main contribution of this work. The proposed model is reliable to identify the main features produced by HIF at different scales of analysis, according to HT and WT. Moreover, the model offers simplicity during its implementation.

The remainder of the paper is organized as follows: Section II introduces the modelling of HIFs on distribution networks and its implementation in ATP/EMTP software. Section III describes the general fundamentals of multiresolution analysis based on WT and HT. Section IV shows the evaluation of the HIF model considering several frequency bands of analysis, as well as a comparison with real data recorded of a HIF signal. Finally, more relevant remarks are presented in the last section.

2. Modelling of HIF for electric distribution networks

2.1. Linear HIF model

To study HIFs, a first approximation considering a pure resistance was initially used. This is a questionable assumption because the asymmetry of the fault currents was neglected [19]. However, this model was adopted for the research of this topic. The main disadvantage of this model is that high impedance faults may be mistaken for load currents. Therefore, transient components may help improve the HIF detection and will have a significant impact on the number of HIF detection.

2.2. Diodes-based model

One of the first models used to study HIFs in electric distribution systems was reported in 1990 [2]. This model was developed from measurements recorded in a 13.8 kV distribution feeder, where the conductor was touching the sandy soil. This has become the most popular model. Fig. 1 shows a simplified model based on two diodes and two d.c. voltage sources connected in antiparallel to obtain the main characteristics of a HIF. Fig. 2(a) and (b) show a typical HIF waveform employing a diodes-based model, where the current asymmetry and the non-linear of voltage-current (V-I) characteristics are observed,

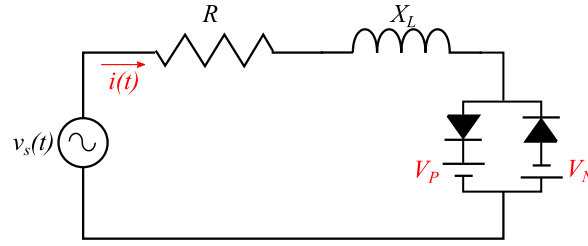


Fig. 1. HIF model based on two diodes.

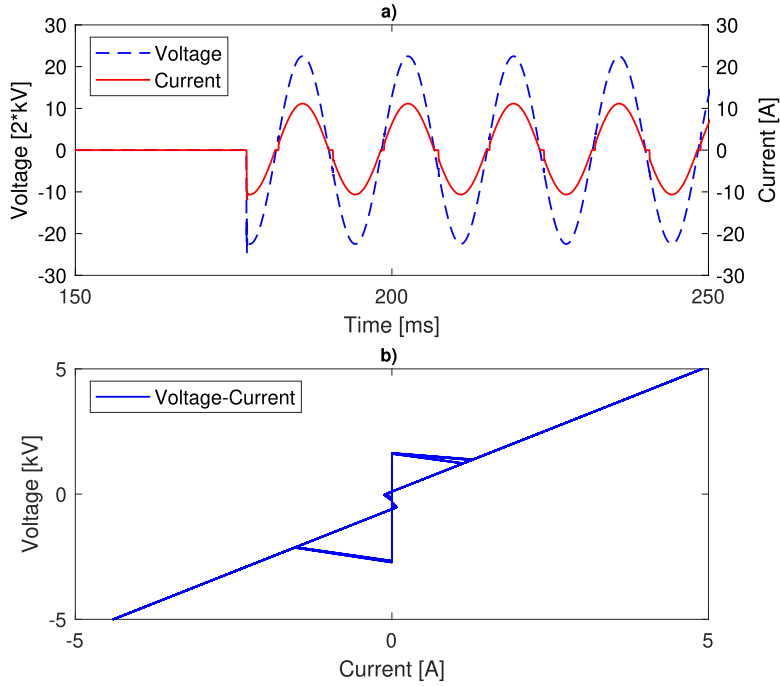


Fig. 2. HIF model: (a) current and voltage signals, (b) V-I characteristics.

respectively. This is the most frequently used model by other researchers in many references such as [7] and [14], and more recently adopted in reference [20]. This model has been widely modified, intending to provide more realistic information about the loop shape non-linearity (V-I characteristic), as well as the asymmetrical shape of the HIF current [21].

2.3. Non-linear resistive-HIF model

According to the above references, the observed characteristics of a HIF can be summarized as follows: low current magnitude due to the soil resistance, a non-linear dependence between voltage and current, and the existence of an electric arc. These characteristics are the base information to develop HIF models, where the electric arc faces new challenges due to its complex nature. Mainly, there are many works focused on modelling the electric arc. For example, black-box models are the most used because they describe the electrical arc characteristics using the provided information by the arc voltage and current signals. Additionally, thermal models have a great history with dynamic arc models, where most of them use the Cassie and Mayr models. Other models are based on the Hochrainer equations to represent the arc, defined by a first-order differential equation. These models and their variations are widely used in the studies concerning the electric arc behaviour, which may be determined by Balestrero et al. [22]:

$$r(t) \frac{d(1/r(t))}{dt} = \frac{1}{\tau} \left(\frac{vi}{P} - 1 \right) \quad (1)$$

where v and i are the arc voltage and current, respectively; $r = v/i$ that is the arc resistance, $\tau(v, i)$ is the time constant of the arc, and $P(v, i)$ is the steady-state arc power.

In this work, the electric arc equation is defined by the Mayr–Cassie formulation and takes the following form:

$$r(t) \frac{d(1/r(t))}{dt} = \frac{1}{\tau} \left(\left(\frac{v}{V_0} \right)^2 - 1 \right) \quad (2)$$

where $r(t)$ is the time-varying arc resistance, V_0 is the steady-state arc voltage and v is the instantaneous arc voltage.

Bear in mind Eq. (2) as well as the differential equation of the resistance, and it is possible to develop a HIF model for distribution networks. For this purpose, the general Eq. (2) may be used, where τ and V_0 are established as constants, giving the following arc equation as a result [23]:

$$\frac{d(1/r(t))}{dt} = \frac{1}{\tau} \left(\frac{1}{R(v)} - \frac{1}{r(t)} \right) \quad (3)$$

where $r(t)$ is the time-varying arc resistance that will define the steady-state resistance. $R(v) = V_0^2 r(t)/v^2$ represents the dynamic term linked to the transient response and τ is the electric arc time constant.

Therefore, the variation of $r(t)$ may be defined by the superposition of a constant part and an oscillating part, as a result:

$$r(t) = R(v) + r'(t) \quad (4)$$

The steady-state of the fault period occurs when $r'(t) = 0$, this means that $r(t) = R(v)$. In consequence, the steady-state resistance R_0 may be found as follows:

$$R_0 = \frac{V_0^2}{v^2} \quad (5)$$

According to (5), v will have a sinusoidal response with a defined frequency $\omega = 2\pi/T$, then, R_0 will be a periodic function of 2ω , bearing in mind that $\tau \gg T/2$, and τ is considered a constant too, so R_0 can be obtained, simplifying the solution. Then, the solution of (3) leads to an expression for representing the dynamic arc resistance in the time domain:

$$r(t) = \frac{R_0}{(1 - e^{-t/\tau})} \quad (6)$$

where R_0 and τ can be obtained by measurements [24].

On the other hand, using t_0 as the time of fault inception, (6) can be rewritten as:

$$r(t) = \frac{R_0}{(1 - e^{-(t-t_0)/\tau})} \quad (7)$$

From the above expressions, it can be observed that $r(t) \rightarrow 0$ when there is an open circuit, this means that there is not a fault at $t - t_0 = 0$. Otherwise, $r(t) \rightarrow R_0$ during the fault period because $t - t_0 = \infty$.

2.3.1. Parameters calculation

The parameters R_0 and τ are computed using the least square method. Denoting $r_f(t_k)$, $i_f(t_k)$, and $v_f(t_k)$ as the resistance, current and voltage, respectively, obtained through measurements at discrete time instants t_1, t_2, \dots, t_M , the arc resistance can be calculated as follows:

$$r_f(t_k) = \sqrt{\frac{\sum_{i=-n}^n v_f^2(t_{k+i})}{\sum_{i=-n}^n i_f^2(t_{k+i})}} \quad (8)$$

where n is the number of samples for a data window of voltage and current signals, normally one cycle of the fundamental frequency.

The theoretical value of the fault resistance $F(R_0, \tau)$ at the discrete-time t_k defined in (6), may be computed using the least-squares method, defined by:

$$F(R_0, \tau) = \sum_{k=1}^N (r(t_k) - r_f(t_k))^2 \quad (9)$$

The minimum value of the sum of squares will be found solving the following system of equations:

$$\frac{\partial(F(R_0, \tau))}{\partial R_0} = 0 \quad (10)$$

$$\frac{\partial(F(R_0, \tau))}{\partial \tau} = 0 \quad (11)$$

After solving Eqs. (10) and (11), the parameters τ and R_0 can be determined employing the electric arc measurements.

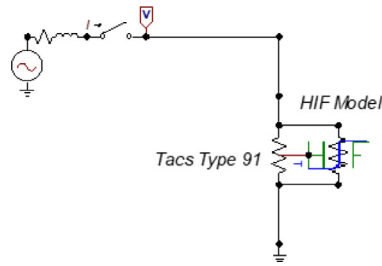


Fig. 3. ATP/EMTP Implementation.

2.3.2. HIF model implementation in ATP/EMTP software

In this subsection, the differential equations that represent the HIF model are solved numerically in the time domain using ATP/EMTP software. Fig. 3 shows the resistive-HIF model implemented in ATP/EMTP using a MODELS language, which interacts with an electric circuit through a Transient Analysis Control System (TACS), resistance type 91. The model allows representing the fault current using the time-varying resistance, defined in (7); the parameters R_0 and τ are calculated for a given surface contact (sod, grass, branch tree, etc.) according to the recorded measurements. The implemented MODEL code is described in Algorithm 1 that gives a resistance value as a result, which varies through time. In order to validate this

Algorithm 1: Resistive-HIF model.

```

Result: Resistance  $r$ 
MODEL HIF model
  INPUT Node1, Node2
  OUTPUT  $r$ 
  DATA  $\tau$ ,  $R_0$ ,  $t_0$ ,  $V_0$ 
  VAR  $V_0$ ,  $v$ ,  $R_{est}$ ,  $R_{dyn}$ ,  $t$ ,  $\tau$ ,  $t_0$ 
  INIT
     $r := R_0$ 
  ENDINIT
  HISTORY  $R_{dyn}$  {dflt:0.0}
  EXEC
    IF  $t > t_0$  THEN
       $v := \text{ABS}(\text{Node1} - \text{Node2})$ 
      IF  $\text{ABS}(v) > 0$  THEN
         $R_{est} := r \times (V_0/v)^2$ 
      ENDIF
      LAPLACE ( $R_{dyn}/R_{est}$ ) := 1.0|/(1.0| +  $\tau$ |s)
       $r := (R_0 + R_{dyn})/(1 - e^{-(t-t_0)/\tau})$ 
    ELSIF  $t < t_0$  THEN
       $r := 1 \times 10^6$ 
    ENDIF
  ENDEXEC
ENDMODEL

```

model, a typical HIF was simulated using the parameters $R_0 = 1000 \Omega$ and $\tau = 0.0298$ s; for instance, Fig. 4(a) shows the HIF voltage and current after the fault inception, while Fig. 4(b) shows the non-linear characteristic, as it was expected, the model is capable of exhibiting low current magnitude in a 13.8 kV distribution system, an asymmetrical current, and the non-linear behaviour. Therefore, it can be emphasized that the model generates a good transient performance, being of easy implementation and versatility. Besides, this model may be assessed considering fewer input parameters than other models such as R_0 and τ , and t_0 to defined the fault inception time.

3. Multiresolution analysis of HIFs

3.1. Wavelet transform

Feature extraction in time-frequency is the key to detect HIFs, and these may be defined according to the produced harmonic components. In general, the features of a HIF signal will define quantitative indexes to identify these kinds of faults. For this purpose, several applications have been developed where DWT has been adopted to extract the time-frequency in-

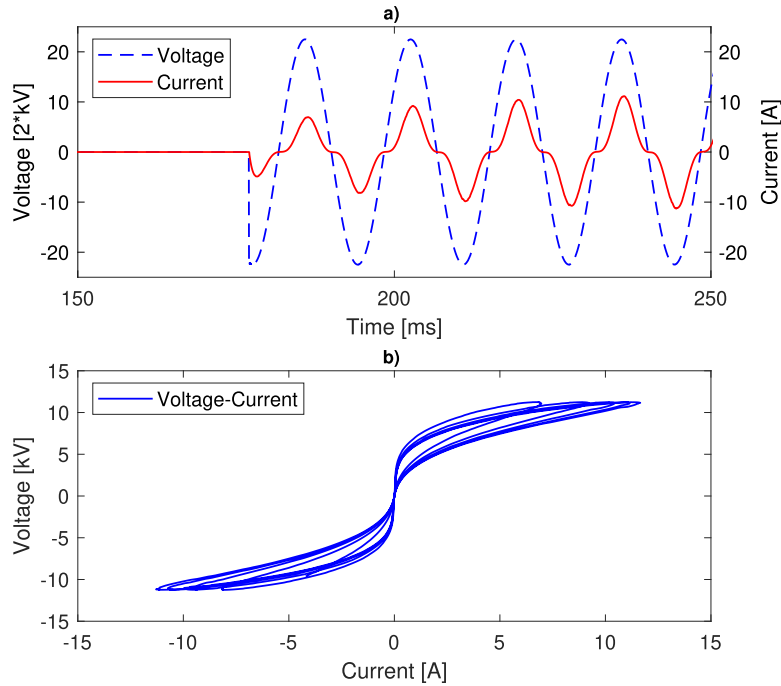


Fig. 4. HIF model: (a) current and voltage signals, (b) V-I characteristics.

formation, which comes from a specific type of failure, in this case, HIFs. Therefore, the HIF model will define the transient components of a HIF signal. Consequently, to avoid errors during the detection, a multiresolution approach is carried out aiming at identifying the best way to analyse HIFs in distribution networks. This is possible considering the high-frequency components generated by a HIF that are represented in the proposed model. For this reason, two HIF models are compared using a multiresolution analysis defined by DWT [20]:

$$DWT(j, k) = \frac{1}{\sqrt{a_0^j}} \sum_i x(i) \psi\left(\frac{k - ia_0^j}{a_0^j}\right) \quad (12)$$

where j represents the scale parameter associated with the frequency, k is a time translation parameter, ψ stands for the mother wavelet.

When DWT is used to carry out multiresolution analysis, its performance links two variables, the mother wavelet selection as well as its decomposition level that is proportional to the sampling frequency. The HIF nature plays an essential role in the mother wavelet selection that can be done using correlation or energy indexes between the analysed signal and the mother wavelet. Besides, to mitigate the effect of the sampling frequency, some researches are focused on studying sampling frequencies of a high order to extract the highest frequency components superimposed during the transient period [25]. Based on the literature, many mother wavelets have been used to detect HIF, but one of the most frequently used is Daubechies family, particularly Daubechies 4 (db4) [16,26]. Therefore, in this work, we will compare the HT with the mother wavelet db4 because it has been stated that it is more adaptable than other mother wavelets. Additionally, different mother wavelets are employed for the same purpose because the mother wavelet selection has been linked to the HIF nature where other wavelets have been used such as Daubechies 5 (db5) [15], Daubechies 10 (db10) [27], Daubechies 14 (db14) [8]. The main goal of using other wavelets is that the mother wavelet selection may affect the algorithm performance of HIF detection, generating the need of use different techniques for analysing HIF signals, as was reported in [10].

3.2. Hermite transform

The Hermite transform in its unidimensional form may extract the features of HIF signals, through a polynomial decomposition within a sliding Gaussian window at overlapping positions along with the time domain. The Hermite polynomials comprise an orthogonal basis within a Gaussian window. This process is a filter-approach that allows computing the polynomial coefficients of the expansion [28]. Moreover, the Gaussian window is the only function that guarantees no spurious artifacts in the resulting convolved signals. The analysis filters are Gaussian derivatives, so the process is equivalent to filter signals with a Gaussian filter followed by computing derivatives of the convolved signal, which are known to be efficient

Table 1
HIF detection based on feature extraction.

| Reference | Features |
|-----------|--------------------------------|
| [4,9,15] | Standard deviation (SD) |
| [5] | Energy (E) |
| [7,13] | Harmonics amplitude |
| [8] | Absolute average value |
| [16] | Average of absolute difference |
| [20,30] | Entropy (H) |
| [27] | Kurtosis index |

feature detectors. By systematically increasing the spread of the Gaussian window, multiscale analysis of the signal can be achieved, allowing the detection of HIFs at different time scales.

In general, an original signal is embedded into a one-parameter family of derived signals, constructed by convolution with Gaussian kernels of increasing width. The Hermite polynomials are defined as:

$$H_n(i) = (-1)^n e^{i^2} \frac{d^n e^{-i^2}}{di^n} \tag{13}$$

where n stands for the n th derivative. For example, the Hermite polynomials for $n=3$, are: $H_0(i) = 1$, $H_1(i) = 2i$, $H_2(i) = 4i^2 - 2$ and $H_3(i) = 8i^3 - 12i$.

As described before, a Gaussian window is used to expand the signal into orthogonal polynomials [29]. Multiplying these polynomials with the Gaussian window, the analysis filters are obtained by:

$$D_n(i) = H_n(-i)g^2(-i) \tag{14}$$

where $g(i)$ is the Gaussian window with standard deviation, σ . Alternatively:

$$D_n(i) = \frac{(-1)^n}{\sqrt{2^n n!}} \frac{1}{\sigma \sqrt{\pi}} H_n\left(\frac{i}{\sigma}\right) e^{-\frac{i^2}{\sigma^2}} \tag{15}$$

Eq. (15) will define the multiresolution approach using HT where the coefficients per scale are obtained:

$$L_n(kT) = \int_{-\infty}^{\infty} x(i)D_n(i - kT)di \tag{16}$$

where $x(i)$ represents the HIF signal, T is the subsampling period, k is the index of the overlapping Gaussian windows, and $L_n(kT)$ is known as forward polynomial transform. Moreover, T is a free parameter with the only requirement that adjacent Gaussian windows overlap given a distance T . If $T = 1$, no subsampling is required and shift invariance is achieved, in contrast to standard wavelet schemes.

The HT is formulated in the continuous domain; therefore, for the case of analyzing discrete signals, a couple of strategies can be followed. The first one consists of discretizing the domain of the filter functions and approximating them by a finite duration impulse function. The disadvantage of this approach is that the signal reconstruction may not be perfect when the inverse Hermite transform is computed. The second strategy adopted consists of using the so-called discrete Hermite transform (DHT) [28]. In this case, the transform is formulated in a discrete space. The discrete counterpart of the Gaussian window is the binomial window. i.e., Eq. (17), for $x = 0, \dots, M$.

$$W^2(x) = \frac{1}{2^M} C_M^x \tag{17}$$

where M is the length of the window and C_M^x will define the discrete Hermite transform.

In general, the discrete orthonormal associated with this window is known as Krawtchouk's polynomials:

$$G_n(x) = \frac{1}{\sqrt{C_M^n}} \sum_{k=0}^n (-1)^{n-k} C_{M-x}^{n-k} C_x^k \tag{18}$$

where $x, n = 0, \dots, M$

$$C_m^n = \frac{n!}{(n-m)!m!} \tag{19}$$

Therefore, for large values of M , the binomial window reduces a Gaussian window, and the Krawtchouk's polynomials turn into the Hermite polynomials. The DHT of order M approximates the continuous Hermite transform of spread $\sigma = \sqrt{M/2}$, being this the main parameter of the DHT that is finite, and M defines the maximum order of the polynomial expansion. The analysis/synthesis process produces the perfect reconstruction of a signal. For this purpose, the filter functions are then defined by:

$$D_n(x) = G_n\left(\frac{M}{2} - x\right)W^2\left(\frac{M}{2} - x\right) \tag{20}$$

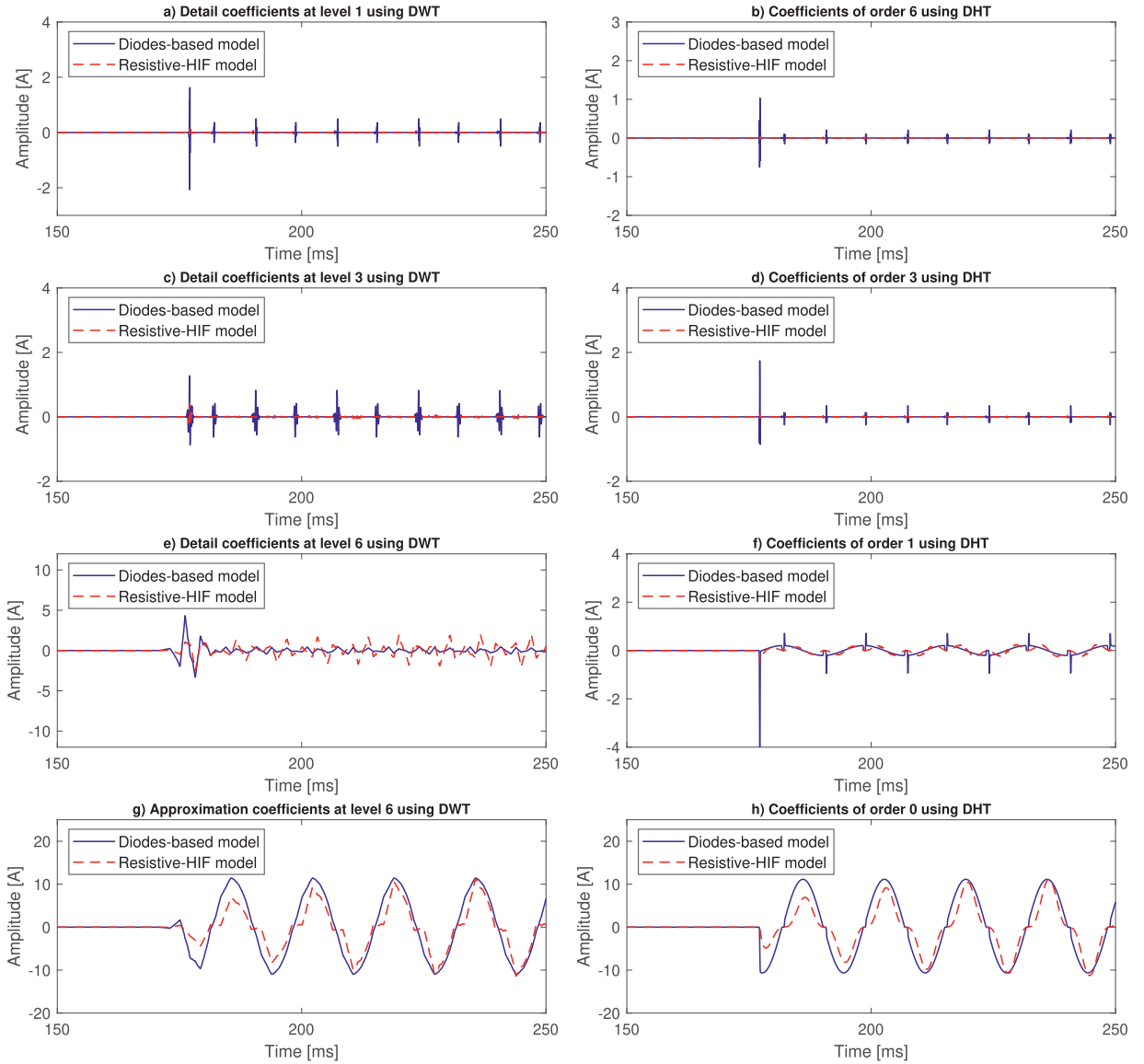


Fig. 5. Multiresolution approach for two different HIF models.

where x takes values between $-M/2$ and $M/2$.

In addition, the multiscale Hermite transform was proposed by Silvan & Escalante [29] that is closely related to the Theory of Scale Space since the HT is based on the analysis of a signal localized by overlapping Gaussian windows. Therefore, an analysis of a signal through the HT at multiple scales is easily achieved by a Hermite polynomial expansion of the localized signal at scale σ :

$$L(x; \sigma) = L(x) * G(x; \sigma) \quad (21)$$

where $G(x; \sigma)$ is the Gaussian analysis function. In the case of the DHT, multiscale analysis is achieved by using binomial windows of different lengths M . The pyramidal implementation of a multiscale Hermite Transform allows to obtain the detailed Hermite coefficients at multiple resolutions; this is done by filtering the low pass coefficients of the previous resolution level, with fixed scale filters (analysis filters) followed by downsampling.

3.3. Feature extraction

The correct selection of feature extraction is not an easy task because it depends on many factors when multiresolution techniques are applied. A proper selection will affect the effectiveness of the classifiers. Therefore, several features have

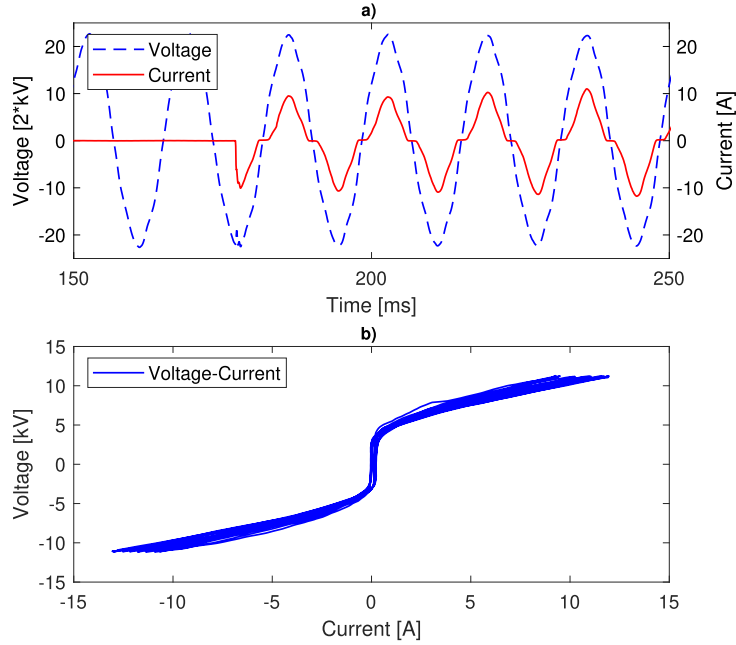


Fig. 6. HIF measurements: (a) current and voltage signals, (b) V-I characteristics.

been employed to detect, locate and classify HIFs in distribution networks. For example, Table 1 shows the most frequently features used for the detection of HIF. They will be discussed in the next section, both to analyse the fault detection and the transient characteristics generated by the proposed model based on a multiresolution analysis.

Based on a multiresolution approach, the feature indexes may be defined for each scale, by the following expressions [30]:

$$SD(j) = \sqrt{\frac{1}{N} \sum_{i=1}^N \left(x(i) - \frac{1}{N} \sum_{i=1}^N x(i) \right)^2} \quad (22)$$

$$E(j) = \frac{1}{N} \sum_{i=1}^N x(i)^2 \quad (23)$$

$$H(j) = \sum_{i=1}^N p_i \ln(p_i) \quad (24)$$

where p_i is defined as

$$p_i = \frac{x(i)^2}{\sum_{i=1}^N x(i)^2} \quad (25)$$

According to the defined features of the studied HIF models, an extensive analysis is carried out using the multiresolution approach. This analysis establishes the advantage of using this kind of analysis, that helps to overcome the limitations when particular HIF models do not reveal an appropriate waveform, or they do not generate sufficient transient frequency components that make more complex the HIF detection.

4. Results and discussions

For validation purposes, a multiresolution pyramidal DHT was used with the following parameters. Binomial window length $M = 8$ and a downsampling factor of 2. This means that the maximum decomposition order is 8 with three pyramidal levels. Also, a comparison is carried out against the DWT, considering the most used wavelet db4. Therefore, different HIF signals will be scaled at different decomposition levels to discover all underlying transient components. The studied signals were analysed using six scales according to DWT; the decomposition will produce detail coefficients per scale and approximation coefficients for the last level. The same process is carried out using DHT considering 1, 2 and 3 scales, but the main difference regarding DWT is that it has eight levels of coefficients per scale plus the lower frequency components corresponding to the zero-derivative.

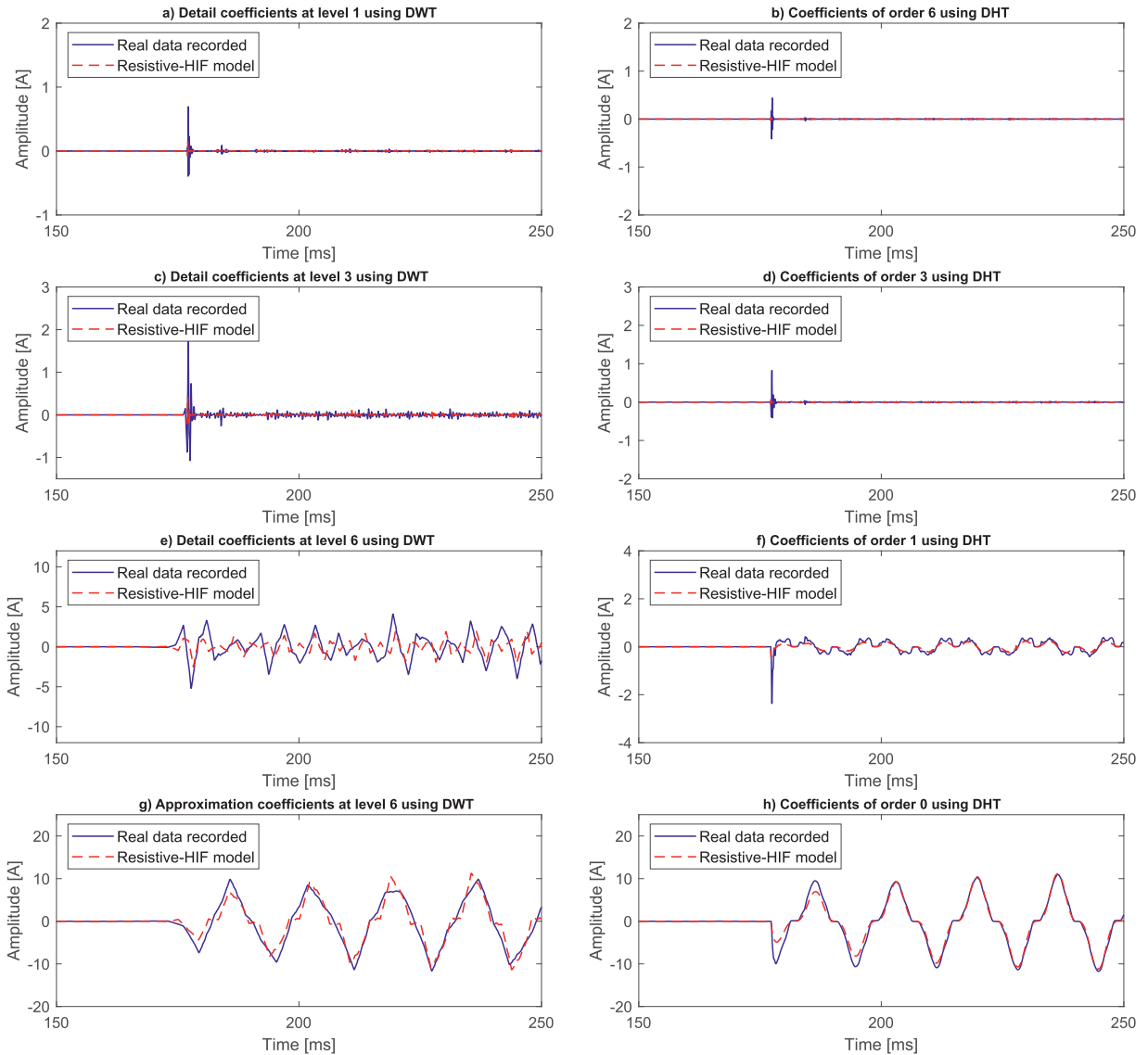


Fig. 7. Multiresolution approach between Resistive-HIF model and measurements.

4.1. Simulations with multiresolution analysis

The proposed model and the diodes-based model are compared using the above described multiresolution approaches. This analysis is the key to detect HIF in distribution systems because it helps to establish the best features to discriminate HIF from slightly load changes, switching capacitor, inrush currents or another kind of small transient perturbation. Fig. 5 shows a comparison at different scales using DWT and DHT. The first level (level 1) corresponds to the highest frequency components of the HIF current, where the detail band of the first resolution level of the WT is shown in 5(a), while the equivalent resolution according to HT corresponds to the coefficients of 6 order, displayed on 5(b). Lower levels in the figure account for deeper detail bands of the WT and lower coefficient orders in the case of the HT. The main differences between these multiresolution approaches appear at the lowest frequencies, as shown in level 6. For the DWT, the level 6 produces approximation and detail coefficients; therefore, to make a comparison in a similar frequency band, the filtering process using the zero-derivative of the Gaussian function according to the Hermite polynomials, will define the approximation coefficients at level 6. Notice that DHT offers multiple resolutions at only one scale, while DWT needs six scales to get the same resolution, being this one of the main advantages of HT over WT; therefore, the computational burden of DWT is higher than DHT. For both studied models, the diodes-based model and the proposed model, it is observed that the major differences, due to the electric arc, occur at level 6 based on the multiresolution analysis because the main activity of the HIF phenomenon appears in that frequency band. Therefore, this study can help to distinguish HIFs from other common

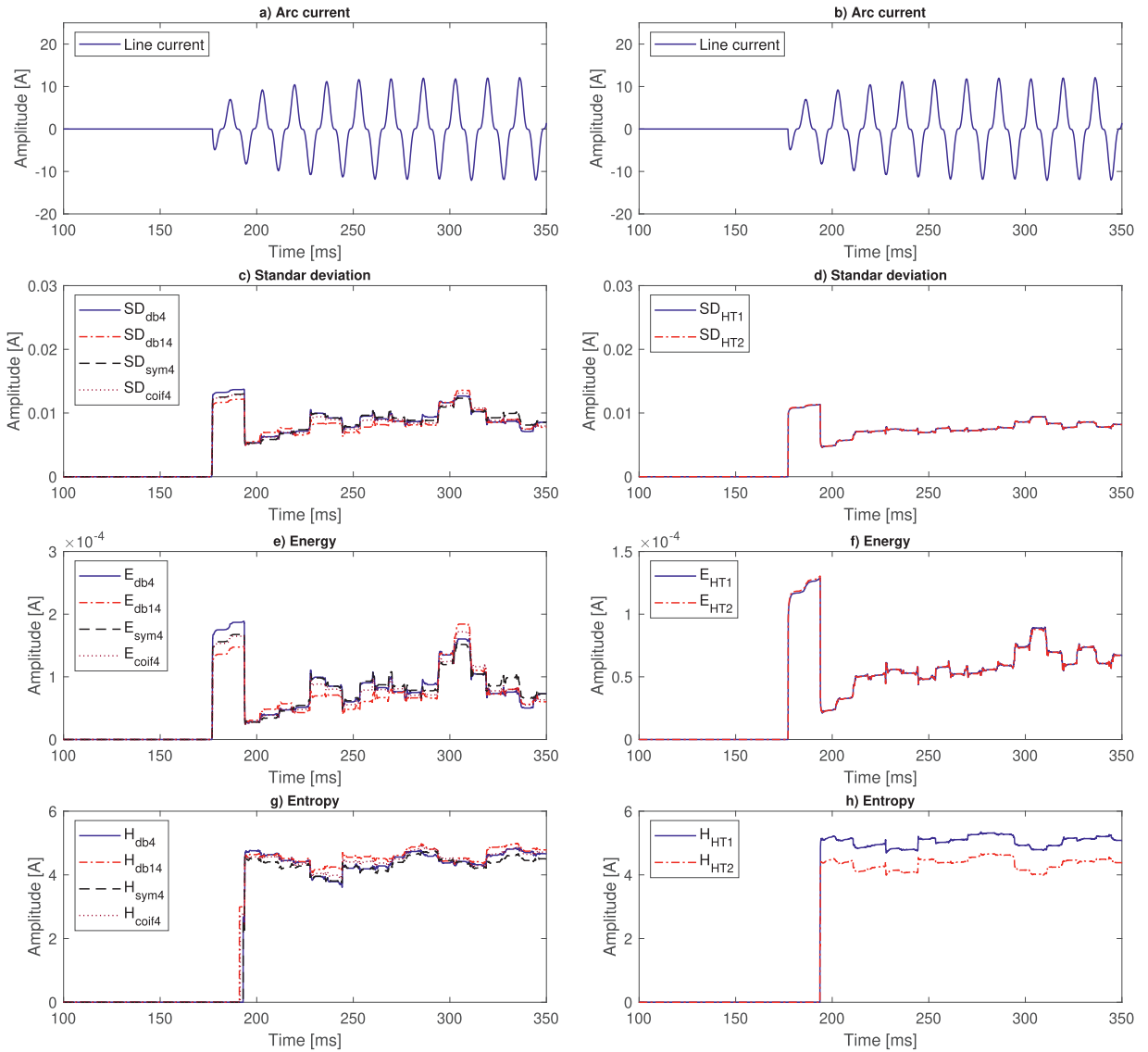


Fig. 8. HIF detection based on feature extraction using DWT and DHT.

transients in distribution systems such as switching capacitors, switching loads, starting motors and inrush transformers currents.

4.2. Multiresolution analysis of real data recorded

On the other hand, a comparison of the Resistive-HIF model was carried out against experimental measurements of a HIF phenomenon obtained from a distribution feeder of 13.8 kV, 60 Hz. The experimental test was carried out in a condition of dry-grass soil in a sunny day, the system is multi-grounded, four wires were utilized with a conductor of 3/0, and the circuit was unloaded [24]; results are displayed on Fig. 6. From 6(a), it is observed a current magnitude less than 10 A that is not enough to operate the protection devices. Moreover, the low current is associated with the high impedance surface, and its variability depends on the non-linear V-I characteristics. Notice that the fault current and the voltage are in phase due to the resistive effect, where the voltage magnitude remains practically constant because the HIF does not represent a load condition in the distribution feeder. The vertical axis on Fig. 6(a) represents both voltage and currents; however, both scales are different, the voltage is close to 10 kV, therefore, a factor 2 is used to compare both signals because the current is around 10 A. Fig. 6(b) shows that the relationship between voltage and current exhibit a non-linear behaviour because of the contact surface on dry-grass.

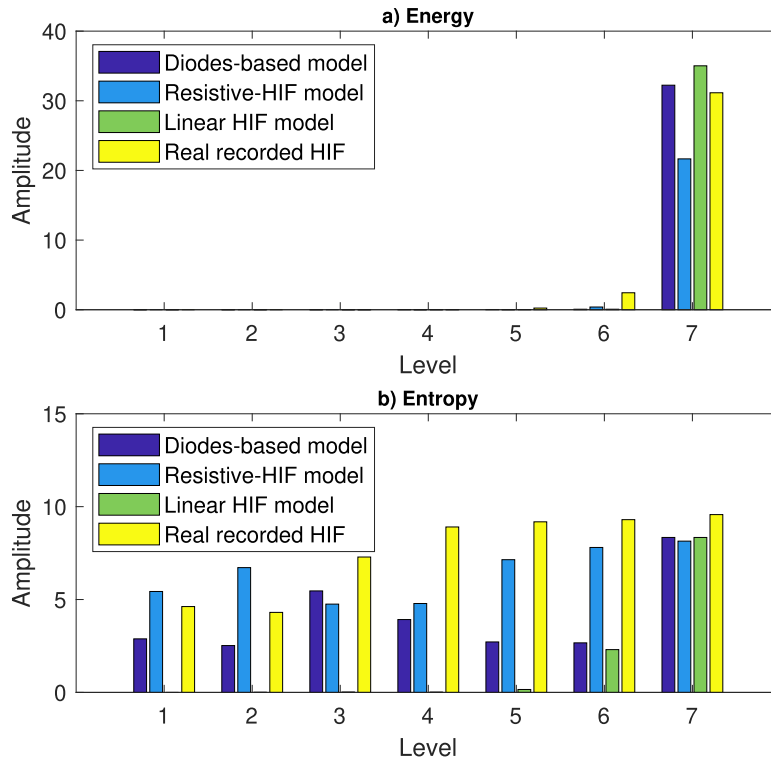


Fig. 9. Comparison between models and data recorded using DWT.

Fig. 7 shows the corresponding comparison using the multiresolution analysis, the arc current behaviour can be observed at the lowest frequency band, which is quite similar between both cases, Resistive-HIF model and measurements based HIF model. Notice that Fig. 7(g) and (h) generate identical results between the proposed model and the acquired measurements during the experiments. In this case, the inception time for the HIF was 177 ms. Based on the multiresolution analysis, the proposed model and the experiments are almost equal after one cycle of the fault occurs, as shown in Fig. 7(h) when DHT is used to compare different levels of interest (frequency bands). A similar effect happened when DWT was used to analyse different scales. Therefore, the measurements of HIF and the proposed model matched one another, where the non-linear resistive characteristics are enough to depict the transient behaviour of HIFs.

4.3. Detection using WT and HT

Detection of HIFs may be carried out analysing the frequency components at different scales. To achieve this, the feature selection will play an important role because a HIF generates transient components at different frequency bands. Therefore, several resolution levels are analysed, for example, Fig. 8 shows a multiresolution with several indexes to quantify the transient components according to DWT and DHT, where transient components will help improve the fault classification regarding other transient phenomena. Fig. 8 shows a comparison with different mother wavelets, where it can be observed substantial differences between every pair of mother wavelets considering various indexes of features. Otherwise, DHT presents a good performance considering two different resolution levels (HT1 and HT2). Based on the results, Fig. 8(c) and (d) show the changes along the time using the standard deviation, while Fig. 8(e) and (f) display the energy results, where the HT present smaller variations along the time than WT, this being an advantage to improve the classification when there are other transient phenomena. Something similar occurs when the entropy is employed in the multiresolution analysis using DWT and DHT; these results are shown in Fig. 8(g) and (h), respectively. Notice that Fig. 8(g) and (h) also show significant changes when the entropy is used for quantifying the transient components. Therefore, to ensure a fair comparison, the energy and entropy will be discussed later, taking into account several scales.

From Fig. 8(d), (f) and (h), it can be noted that the transient components can be detected at different pyramidal levels in several coefficient orders according to the HT. The lower resolution level, the lower the coefficient order in which the transient response is higher. Moreover, even in the same resolution level, not all coefficient orders respond to the transient in the same way. The transient response is higher when the transient waveform is more similar to the corresponding filter profile, i.e. when there is a resonance between the transient response and the filter profile. This is a clear advantage of the HT over other multiresolution schemes such as wavelets, because wavelets may need an additional process to identify which

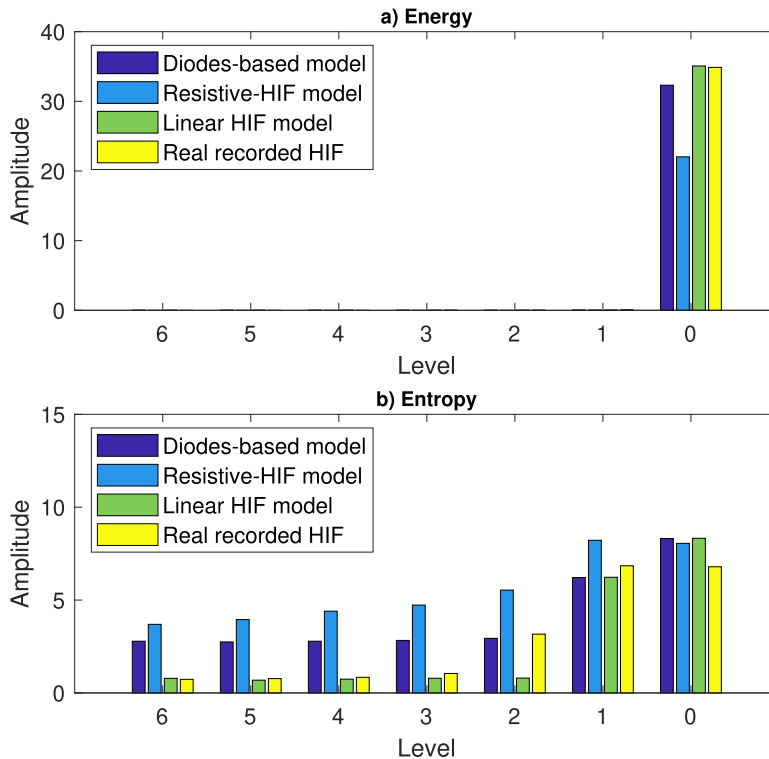


Fig. 10. Comparison between models and data recorded using DHT.

mother wavelet is the best for a specific application, i.e., in the latter multiresolution analysis is based on signal analysis with dilated versions of the same mother wavelet, while in the former multiple filter functions profiles are used at each resolution level. This increases the opportunity to find a filter function at some resolution level that matches the transient and produces a larger signal-noise ratio (SNR) filter responses.

4.4. Comparison of models based on multiresolution approaches

Fig. 9(a) and (b) show the characteristics of HIFs by employing the energy and the entropy, respectively. In these figures, three different models (diodes-based model, resistive-HIF model, linear HIF model) are analysed and compared against real measurements. Fig. 9(a) presents the most relevant activity of the electric arc at levels 6 and 7, when the energy is used to extract the main characteristics of this kind of events, which correspond to the approximation and detail coefficients at level 6, respectively. In the same way, the entropy generates significant differences at different levels of analysis, showing significant differences in all levels according to the analysed models by using DWT, as presented in Fig. 9(b).

On the other hand, Fig 10(a) and (b) show the energy and the entropy when the multiresolution approach is carried out using HT. From these results, it can be observed a quite similar behaviour compared with the obtained results by the DWT. Especially, at levels 0 and 1 (lower frequency components corresponding to level 6 according to the DWT), where the entropy is more representative to detect the activity of the electric arc in all decomposition levels. Therefore, entropy is a more suitable feature of HIF that facilitates fault detection. This occurs when HT and DWT are used to extract all transient characteristics.

5. Conclusion

An in-depth analysis of different high impedance fault models was carried out, aiming to represent and quantify the transient-state and the steady-state frequency components of high impedance fault signals. The non-linear resistive model was compared against other well-accepted models, where their parameter may be computed employing measurements, that are not always available. Therefore, to overcome these drawbacks, a simplified model was developed with a single non-linear resistance that was capable of preserving the essential characteristics of high impedance faults. The presented model is based on the arc model theory and is validated with multiresolution analysis. The proposed model demonstrates versatility, simplicity, and it can be easily implemented.

On the other hand, wavelet transform and Hermite transform allow finding out the main differences between several models according to the multiresolution analysis. This analysis demonstrates that the high impedance fault detection may

be identified under specific frequency bands; the techniques were used to analyse the diodes-based model, linear model and the proposed model, where similar results were observed. Finally, the results showed that the entropy and the energy for several high impedance fault models and measurements, present the significant differences at levels 6 and 7, giving an indicative of high impedance fault when both techniques are used. Finally, the Hermite transform offers a filter function for each resolution that matches the transient waveform of the analysed signal.

Declaration of Competing Interest

The authors declare that they have no known competing financial interests or personal relationships that could have appeared to influence the work reported in this paper.

CRedit authorship contribution statement

Vicente Torres-Garcia: Conceptualization, Formal analysis. **Daniel Guillen:** Methodology, Formal analysis. **Jimena Olveres:** Formal analysis, Conceptualization. **Boris Escalante-Ramirez:** Formal analysis, Validation. **Juan R. Rodriguez-Rodriguez:** Conceptualization, Formal analysis.

Acknowledgements

Vicente Torres G., Boris Escalante-Ramírez and Jimena Olveres wish to thank UNAM PAPIIT grants IA106420, IN116917 and IA103119, respectively.

Supplementary material

Supplementary material associated with this article can be found, in the online version, at doi:[10.1016/j.compeleceng.2020.106576](https://doi.org/10.1016/j.compeleceng.2020.106576).

References

- [1] Report of PSRC working group D15, 'High impedance fault detection technology'. 1996. <http://grouper.ieee.org/groups/td/dist/documents/highz.pdf>.
- [2] Emanuel AE, Cyganski D, Orr JA, Shiller S, Gulachenski EM. High impedance fault arcing on sandy soil in 15 KV distribution feeders: contributions to the evaluation of the low frequency spectrum. *IEEE Trans Power Deliv* 1990;5(2):676–86.
- [3] Iurinic LU, Herrera-Orozco AR, Ferraz RG, Bretas AS. Distribution systems high-impedance fault location: A parameter estimation approach. *IEEE Trans Power Deliv* 2016;31(4):1806–14.
- [4] Chaitanya B, Yadav A. An intelligent fault detection and classification scheme for distribution lines integrated with distributed generators. *Comput Electr Eng* 2018;69:28–40.
- [5] Santos WC, Lopes FV, Brito NSD, Souza BA. High-impedance fault identification on distribution networks. *IEEE Trans Power Deliv* 2017;32(1):23–32.
- [6] Darwish HA, Elkalashy NI. Universal arc representation using EMTP. *IEEE Trans Power Deliv* 2005;20(2):772–9.
- [7] Samantaray S, Dash P, Upadhyay S. Adaptive kalman filter and neural network based high impedance fault detection in power distribution networks. *Int J Electr Power Energy Syst* 2009;31(4):167–72.
- [8] Elkalashy NI, Lehtonen M, Darwish HA, Taalab A-MI, Izzularab MA. Dwt-based extraction of residual currents throughout unearthened MV networks for detecting high-impedance faults due to leaning trees. *Eur Trans Electr Power* 2007;17(6):597–614.
- [9] Chen J, Phung T, Blackburn T, Ambikairajah E, Zhang D. Detection of high impedance faults using current transformers for sensing and identification based on features extracted using wavelet transform. *IET Gener Trans Distrib* 2016;10(12):2990–8.
- [10] Cheng J-Y, Huang S-J, Hsieh C-T. Application of Gabor–Wigner transform to inspect high-impedance fault-generated signals. *Int J Electr Power Energy Syst* 2015;73:192–9.
- [11] Gautam S, Brahma SM. Detection of high impedance fault in power distribution systems using mathematical morphology. *IEEE Trans Power Syst* 2013;28(2):1226–34.
- [12] Soheilil A, Sadeh J. Evidential reasoning based approach to high impedance fault detection in power distribution systems. *IET Gener Trans Distrib* 2017;11(5):1325–36.
- [13] Samantaray S. Ensemble decision trees for high impedance fault detection in power distribution network. *Int J Electr Power Energy Syst* 2012;43(1):1048–55.
- [14] Milioudis AN, Andreou GT, Labridis DP. Detection and location of high impedance faults in multiconductor overhead distribution lines using power line communication devices. *IEEE Trans Smart Grid* 2015;6(2):894–902.
- [15] Baqui I, Zamora I, Mazn J, Buigues G. High impedance fault detection methodology using wavelet transform and artificial neural networks. *Electr Power Syst Res* 2011;81(7):1325–33.
- [16] Bakar A, Ali M, Tan C, Mokhlis H, Arof H, Illias H. High impedance fault location in 11KV underground distribution systems using wavelet transforms. *Int J Electr Power Energy Syst* 2014;55:723–30.
- [17] Vianna JTA, Araujo LR, Penido DRR. High impedance fault area location in distribution systems based on current zero sequence component. *IEEE Latin Am Trans* 2016;14(2):759–66.
- [18] Mortazavi SH, Moravej Z, Shahrtash SM. A searching based method for locating high impedance arcing fault in distribution networks. *IEEE Trans Power Deliv* 2019;34(2):438–47.
- [19] Carr J. Detection of high impedance faults on multi-grounded primary distribution systems. *IEEE Trans Power Appar Syst* 1981;PAS-100(4):2008–16.
- [20] Gomes DPS, Ozansoy C, Ulhaq A. High-sensitivity vegetation high-impedance fault detection based on signal's high-frequency contents. *IEEE Trans Power Deliv* 2018;33(3):1398–407.
- [21] Zamanan N, Sykulski JK. Modeling an arcing high impedances fault based on the physical process involved in the arc. In: *Proceedings of the 6th WSEAS. Lisboa, Portugal; 2006. p. 28–33.*
- [22] Balestrero A, Ghezzi L, Popov M, van der Sluis L. Current interruption in low-voltage circuit breakers. *IEEE Trans Power Deliv* 2010;25(1):206–11.
- [23] Kizilcay M, Pniok T. Digital simulation of fault arcs in power systems. *Eur Trans Electr Power* 1991;1(1):55–60.
- [24] Torres V, Guardado J, Ruiz H, Maximov S. Modeling and detection of high impedance faults. *Int J Electr Power Energy Syst* 2014;61:163–72.
- [25] Gomes DP, Ozansoy C, Ulhaq A, de Melo Vieira JAnior JC. The effectiveness of different sampling rates in vegetation high-impedance fault classification. *Electr Power Syst Res* 2019;174:105872.

- [26] Mohammadnayan Y, Amraee T, Soroudi A. Fault detection in distribution networks in presence of distributed generations using a data mining-driven wavelet transform. *IET Smart Grid* 2019;2(2):163–71.
- [27] Wang X, Gao J, Wei X, Song G, Wu L, Liu J, et al. High impedance fault detection method based on variational mode decomposition and Teager-Kaiser energy operators for distribution network. *IEEE Trans Smart Grid* 2019;10(6):6041–54.
- [28] Martens J. The hermite transform-theory. *IEEE Trans Acoust Speech Signal Process* 1990;38(9):1595–606.
- [29] Silvan-Cardenas JL, Escalante-Ramirez B. The multiscale hermite transform for local orientation analysis. *IEEE Trans Image Process* 2006;15(5):1236–53.
- [30] Sekar K, Mohanty NK. Data mining-based high impedance fault detection using mathematical morphology. *Comput Electr Eng* 2018;69:129–41.

Vicente Torres-García was born in Morelia, Michoacán, Mexico. He received the M.Sc. and Ph.D. degrees in electrical engineering from the Instituto Tecnológico de Morelia in 2009 and 2015, respectively. He is currently with the Department of Electrical Energy at Universidad Nacional Autónoma de México. His research interests include power systems, distribution networks, electromagnetic transients and power system protection.

Daniel Guillen received the B.Eng. degree from Instituto Tecnológico de Morelia, México, in 2007, his M.Sc. and Ph.D. degrees from Universidad Autónoma de Nuevo León, México, in 2010 and 2015, respectively. He is currently with Tecnológico de Monterrey. His main research interests are power system protection, wide-area monitoring, signal processing and transient analysis.

Jimena Olveres is with Universidad Nacional Autónoma de México (UNAM). She received her B.S. degree in Biomedical Engineering from Universidad Iberoamericana in México city, a Master in Engineering and a Ph.D. in Computer Science from UNAM. Her research areas include computational models for image processing, machine learning for computer vision, specializing in medical image analysis.

Boris Escalante-Ramirez is with Universidad Nacional Autónoma de México. He received a Ph.D. from the Technical University of Eindhoven (1992). His research areas include computational models for image processing and computer vision.

Juan R. Rodríguez-Rodríguez received the B.Eng. and Ph.D. degrees in electrical engineering from the Instituto Tecnológico de Morelia, Morelia, México, in 2009 and 2015, respectively. He is currently with the Department of Electrical Energy at UNAM, México. His current research interests include power electronics converters, smart-grids, and renewable energy.